LONG-TERM MONITORING STRATEGY FOR CONCRETE-BASED STRUCTURES USING NONLINEAR KALMAN FILTERING

K.A. Snyder[1], Z.Q. Lu[1], and J. Philip[2]
[1] National Institute of Standards and Technology, Gaithersburg, MD USA
[2] U.S. Nuclear Regulatory Commission, Rockville, MD USA

ABSTRACT

Kalman filtering is introduced as a rational means for developing a monitoring strategy for concrete structures. The mathematics and utility of linear Kalman filters are presented briefly, and the use of linear filters is demonstrated for Fickian diffusion. The nonlinear extended Kalman filter is introduced and its utility in estimating a transport parameter is demonstrated. The concrete service life computer program 4SIGHT is introduced briefly and combined with nonlinear filtering to refine the transport coefficient from a laboratory diffusion experiment. A fictitious monitoring strategy is presented that uses Kalman filtering to both refine estimates and extend the time between monitoring intervals. The advantages of using Kalman filtering, along with the remaining technical difficulties, are discussed.

Keywords: concrete; Kalman filter; monitoring; performance assessment; service life.

1 - INTRODUCTION

Virtually all failures of concrete structures can be attributed to chemical attack, either from without (sulfate attack, corrosion of the steel reinforcement, etc.) or from within the structure (alkali silica, etc.). The specific degradation mechanism causing the failure may be either unforeseen or the rate of advancement may be underestimated. Most concrete structures in the United States are still designed and built using historical knowledge that has been tabulated in engineering manuals of practice, which do not address a specific structure and its environment. Computer models exist for predicting concrete performance based on the cement properties, the concrete mixture design, and the structure's environment. Unfortunately, these models are used in only a small fraction of new construction.

The best of these computer models have achieved an adolescent stage of development; they are technically sophisticated but still have not incorporated all the complexity of concrete. Given this stage of technical advancement in concrete service life models, it is unreasonable to expect any model to accurately predict performance with a high degree of certainty, especially over very long time scales (e.g., centuries or millennia). By analogy, a Professional Engineer (PE) will sign the drawings of a structural design, thereby staking his or her professional reputation on the structural performance. It would be rare, however, for a concrete materials engineer to stake their reputation by signing a corresponding statement of durability that a concrete structure will achieve the design service life.

This state of technical achievement is an important point for the construction of critical infrastructure concrete components. If there are no computer models that are absolutely reliable, the only sensible alternative is to develop a supplemental monitoring strategy. Ideally, this strategy would combine both computer model predictions and periodic measurements. Kalman filtering [1] is one way to mathematically combine such data. Moreover, the technique is optimized so that after combining both the model prediction and the physical measurement, the uncertainty is less than that for either one individually. This idea is not new. Kalman filtering has already been incorporated into hydrogeological modeling [2, 3] and the study of porous building materials [4].

The Kalman filter is introduced and applied to various artificial scenarios. The linear filter is applied to a Fickian diffusion problem. The nonlinear filter is introduced as a means of parameter estimation in Fickian problems. The 4SIGHT computer model is introduced to highlight constraints that may arise in using Kalman filters with computer service life models for concrete. A fictitious monitoring scenario is presented to demonstrate how Kalman filtering may extend the time between measurements and simultaneously reduce uncertainty.

2 - LINEAR KALMAN FILTER

Let there be a vector $\mathbf{x}$ that is a list $\{x_0, x_1, \ldots, x_n\}$ of all the quantities (internal field variables, transport parameters, etc.) that a performance assessment model needs to predict the future time-dependent behavior of a system. In addition, there may also be external control variables $\mathbf{u}$. For a linear model, the vector advances from time t_{k-1} to time t_k, by a linear transformation from $\mathbf{x}^{k-1}$ to $\mathbf{x}^k$ effected by a matrix propagator A. If the transformation is a

linear approximation to a continuum problem, there may be model error $\mathbf{q}$ introduced into the answer:

$$\mathbf{x}^k = \mathsf{A}_k \mathbf{x}^{k-1} + \mathsf{B}_k \mathbf{u}^{k-1} + \mathbf{q}^{k-1} \tag{1}$$

The process error vector $\mathbf{q}$ does not include uncertainties in either the state vector or the transformation matrix $\mathsf{A} \in \mathbb{R}^{n \times n}$.

There are measurements $\mathbf{y} = \{y_0, y_1, \ldots, y_m\}$ taken at each t_k that characterize important properties of the system. These properties are a function of the state vector $\mathbf{x}$ at t_k. For the linear model, the predicted outcomes of these measurements can be expressed as a linear function of the state vector $\mathbf{x}$:

$$\mathbf{y}^k = \mathsf{J}_k \mathbf{x}^k + \mathbf{r}^k \tag{2}$$

The matrix $\mathsf{J} \in \mathbb{R}^{m \times n}$ converts state vector quantities to measured quantities, and the vector $\mathbf{r}$ represents the measurement uncertainty. The vectors $\mathbf{q}$ and $\mathbf{r}$ are assumed to represent errors having zero mean, and are characterized by covariance matrices Q and R, respectively, and cannot account for inherent bias in a model.

In practice, the filter works by first advancing the process model to obtain a best model estimate and then correcting this estimate based on the measurements. The state vector advanced to the point of just prior to the measurement is denoted by $\hat{\mathbf{x}}^{k_-}$, and the estimated measurement value $\hat{\mathbf{y}}^k$ is based on this value:

$$\hat{\mathbf{x}}^{k_-} = \mathsf{A}_k \hat{\mathbf{x}}^{k-1} + \mathsf{B}_k \mathbf{u}^{k-1} \tag{3}$$

$$\hat{\mathbf{y}}^k = \mathsf{J}_k \hat{\mathbf{x}}^{k_-} \tag{4}$$

The notation used here is that discrete time is denoted in vectors with a superscript, and in matrices by a subscript. The vector superscript denotes instantaneous time, and the matrix subscript denotes the time to which it propagates a vector. The superscript k_- denotes the time up to but just before the measurement at time t_k. The filtering outlined below advances the state vector from state k_- to time t_k.

At this point, Kalman filtering is used to obtain an adjusted state vector $\mathbf{x}^k$ that minimizes the uncertainty. The prediction error covariance matrix P, which characterizes uncertainty in the state vector, is also advanced to the time just before the measurement:

$$\mathsf{P}_{k_-} = \mathsf{A}_k \mathsf{P}_{k-1} \mathsf{A}_k^{\mathrm{T}} + \mathsf{Q}_k \tag{5}$$

It is then used to calculate the Kalman gain matrix K_k:

$$\mathsf{K}_k = \mathsf{P}_{k_-} \mathsf{J}_k^{\mathrm{T}} \left(\mathsf{J}_k \mathsf{P}_{k_-} \mathsf{J}_k^{\mathrm{T}} + \mathsf{R}_k \right)^{-1} \tag{6}$$

Finally, the state vector $\mathbf{x}$ and the error covariance matrix P are advanced to the time of just after the measurement:

$$\hat{\mathbf{x}}^k = \hat{\mathbf{x}}^{k_-} + \mathsf{K}_k \left[\mathbf{y}^k - \mathsf{J}_k \hat{\mathbf{x}}^{k_-} \right] \tag{7}$$

$$\mathsf{P}_k = \mathsf{P}_{k_-} - \mathsf{K}_k \left[\mathsf{J}_k \mathsf{P}_{k_-} \mathsf{J}_k^{\mathrm{T}} + \mathsf{R}_k \right] \mathsf{K}_k^{\mathrm{T}} \tag{8}$$

Note that the gain matrix K_k looks something like $\mathsf{P}_{k_-} / \left(\mathsf{P}_{k_-} + \mathsf{R}_k \right)$. In effect, it varies from zero (large measurement uncertainty) to one (large process uncertainty). More thorough discussions of Kalman filtering can be found elsewhere [5].

3 - FICKIAN DIFFUSION

The linear Kalman filter is first applied to an example that is based on Fickian diffusion. The underlying process satisfies Fick's law relating flux $\mathbf{j}$ and concentration c via the diffusion coefficient D:

$$\frac{\partial c}{\partial t} = D \nabla^2 c \tag{9}$$

For this example, D is assumed to be constant in both space and time.

The process model is a matrix equation for $c(x,t)$ along a one-dimensional lattice, as shown in Fig. 1. The process state vector $\mathbf{x} = \{x_0, x_1, \ldots, x_N\}$ represents the concentration at each node at a particular time. The distance between nodes is Δx and the total length $L = N\Delta x$.

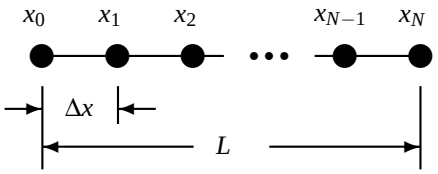

Figure 1: Schematic of a one-dimensional diffusion problem.

The boundary and initial conditions are chosen so as to simplify the problem. Initially, the concentration at all but element x_0 is zero. The boundary conditions are constants:

$$x_0 = C \qquad\qquad x_N = 0$$

The quantity x_0 is included in the state vector so that the external concentration can be treated as an observed quantity. The quantity x_N is treated as a constant equal to zero, and is omitted from the state vector, thereby giving x_0 the significance of representing the concentration difference across the system of length L.

The time-dependent behavior of the state variable $\mathbf{x}$ is calculated using the the Crank-Nicholson algorithm, which is unconditionally stable [6]. The resultant process model is a linear matrix equation:

$$\mathbf{x}^k = \mathsf{A}\,\mathbf{x}^{k-1} \tag{10}$$

The propagator matrix A is a function of the dimensionless parameter η:

$$\eta = \frac{D\,\Delta t}{(\Delta x)^2} \tag{11}$$

The parameter η is both a dimensionless time and a dimensionless diffusion coefficient in this discussion. In this linear example, however, the Δt are constant. Over the course of a calculation, the matrix A is a constant. It does, however, vary among ensemble realizations, for it incorporates parameter uncertainty in the diffusion coefficient embedded within η.

The monitoring will consist of measurements taken at depths of 0, $L/4$, $L/2$, and $3L/4$. The number N of computational nodes is chosen to be divisible by four. As a result, the elements of the matrix J_k are 1 along the four diagonal elements corresponding to the location of the measurements, and zero otherwise.

As this is a fictitious example, there are no measured concentrations. As an alternative, measurements are calculated using the analytical solution for the system having concentration $c(0,t) = C$ and $c(L,t) = 0$ [7]:

$$c(v\Delta x, t_k) = C\left\{1 - \frac{v\Delta x}{L} - \frac{2}{\pi}\sum_{n=1}^{\infty}\frac{1}{n}\sin\frac{n\pi x}{L}\exp\left[-\left(\frac{k\eta}{N^2}\right)n^2\pi^2\right]\right\} \tag{12}$$

The quantity $v\,\Delta x$ is the location of both the computational node and the measurement, and the ratio $(k\eta/N^2)$ represents the total elapsed time in dimensionless scale invariant units.

The true measured values are calculated using Eq. 12 for each of the four locations. To this true value, a random Gaussian deviate, with mean zero and standard deviation σ_m, is used to generate a value for the measurement vector $\mathbf{y}$.

The starting parameters, denoted true values with a subscript "T", for the calculation are as follows:

$$C_T = 1 \qquad \sigma_m = 0.05 \qquad \eta_T = 0.80 \qquad \sigma_\eta = 0.16 \tag{13}$$

The true values C_T and η_T are used in Eq. 12 above for generating measurement values. For the purpose of filtering, however, it is assumed that the true value of diffusion coefficient within η_T is not known, and that a measurement is needed to determine an initial value. This value is calculated using η_T and a Gaussian random deviate with mean zero and standard deviation σ_η; in this example, $\eta = 0.9140$ and is constant for the duration of the calculation. This initial value of η is used in the propagator matrix A.

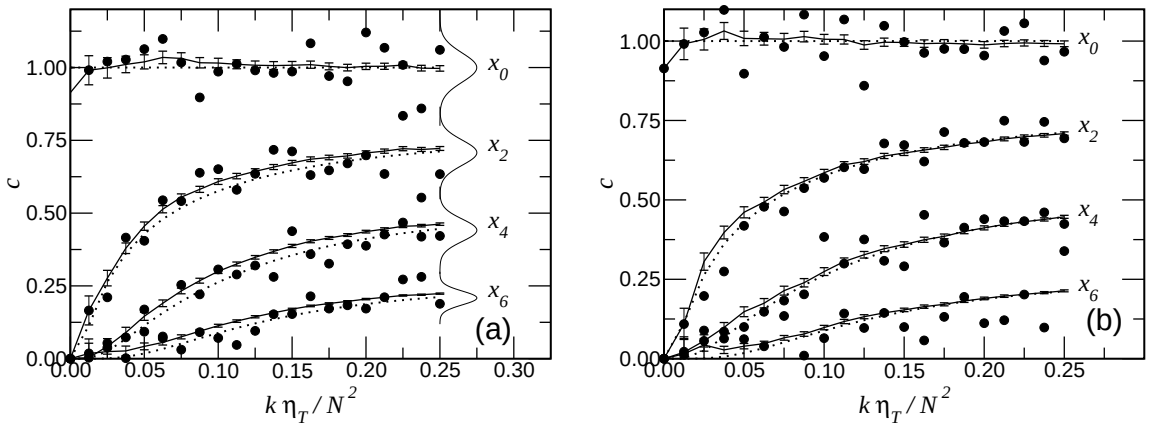

Figure 2: Measured (filled circles) and filtered (solid line with error bars) concentration c as a function of scaled time $k\eta_T/N^2$. The true values are denoted by the dotted line. (a) Linear filtering with no parameter estimation. (b) Nonlinear filtering with parameter estimation. The initial values are $\eta = 0.9867$ and $C = 0.9140$.

The results of the calculation are shown in Fig. 2(a) for the parameter values given in Eq. 13, and $N = 8$. (Note that the initial values were $\eta = 0.9867$ and $C = 0.9140$.) The measured values, calculated using Gaussian random deviates, are shown as solid circles in the graph. The filtered prediction is depicted by the solid line, with error bars denoting one standard deviation. The true values are denoted by the dotted lines. The discrepancy between the filtered values and the true values is due to the +23 % initial error in the coefficient η. Unfortunately, filtering the concentrations alone cannot overcome the underlying problem of initially overestimating the transport coefficient. Incorporating parameter estimation will require nonlinear Kalman filtering.

Also shown in Fig. 2(a) are Gaussian curves denoting measurement and model uncertainty in the absence of filtering. The Gaussian near the label x_0 represents the measurement uncertainty σ_m. The other three Gaussians denote the variation in the concentrations at dimensionless time $k\eta_T/N^2 = 0.25$ that are calculated using random initial values for C and η. The error bars for the filtered values are considerably smaller than either the measurement or the model output uncertainties.

4 - EXTENDED KALMAN FILTER

Nonlinear Kalman filters are designed for process and measurement models that cannot be expressed in the form of Eqs. 1 and 2. More generally, nonlinear model predictions are expressed as functions of the predicted state vector $\hat{\mathbf{x}}$ and the control vector $\mathbf{u}$:

$$\hat{\mathbf{x}}^{k-} = \mathbf{f}\left(\hat{\mathbf{x}}^{k-1}, \mathbf{u}^{k-1}\right) \tag{14}$$

$$\hat{\mathbf{y}}^{k} = \mathbf{g}\left(\hat{\mathbf{x}}^{k-}\right) \tag{15}$$

The notation $\mathbf{f}()$ and $\mathbf{g}()$ denotes a function that returns a vector. From here, one can choose among extended [8], unscented [9], and ensemble [10] Kalman filtering. Here, the extended method is described and used.

The extended Kalman filter (EKF) simplifies the nonlinear problem by linearizing the model near the prediction point, and assuming that the errors in close proximity to the best guess are roughly Gaussian. The linearization uses the Jacobian matrices $\mathbb{F}$ and $\mathbb{G}$:

$$\begin{aligned} \mathbb{F} &= \frac{\partial \mathbf{f}}{\partial \mathbf{x}} & \mathbb{F}_{ij} &= \frac{\partial f_i}{\partial x_j} \\ \mathbb{G} &= \frac{\partial \mathbf{g}}{\partial \mathbf{x}} & \mathbb{G}_{ij} &= \frac{\partial g_i}{\partial x_j} \end{aligned} \tag{16}$$

For the purely linear process model satisfying Eq. 1, $\mathbb{F} = \mathsf{A}$ and $\mathbb{G} = \mathsf{J}$.

The Jacobian is the linearization about the best guess, and is used to update the error covariance matrices:

$$\mathsf{P}_{k-} = \mathbb{F}_k \mathsf{P}_{k-1} \mathbb{F}_k^{\mathrm{T}} + \mathsf{Q}_k \tag{17}$$

The remainder of the filter remains conceptually identical to the linear filter:

$$\mathsf{K}_k = \mathsf{P}^{k-}\,\mathbb{G}^{\mathrm{T}}\left(\mathbb{G}_k\,\mathsf{P}^{k-}\,\mathbb{G}_k^{\mathrm{T}}+\mathsf{R}_k\right)^{-1} \tag{18}$$

$$\mathsf{P}_k = \mathsf{P}_{k-}-\mathsf{K}_k\left[\mathbb{G}_k\,\mathsf{P}_{k-}\,\mathbb{G}_k^{\mathrm{T}}+\mathsf{R}_k\right]\mathsf{K}_k^{\mathrm{T}} \tag{19}$$

$$\hat{\mathbf{x}}^k = \hat{\mathbf{x}}^{k-}+\mathsf{K}_k\left[\mathbf{y}-\mathbf{g}(\hat{\mathbf{x}}^{k-})\right] \tag{20}$$

This linearization of the nonlinear model is accurate for process models with weak nonlinearity. As the possibility for noticeable nonlinearity between measurements increases, the error covariance matrix underestimates the uncertainty.

5 - TRANSPORT COEFFICIENT ESTIMATION

In the previous Fickian diffusion example, the diffusion coefficient was incorporated into the parameter η. To obtain an optimal estimation of η, the state vector $\mathbf{x}$ is expanded to include the parameter η:

$$\mathbf{x}^{\mathrm{T}} = [C, x_1, x_2, \ldots, x_{N-1}, \eta] \tag{21}$$

Although the addition of the parameter η into the state vector makes this a nonlinear filter problem, the pre-filtered estimate $\hat{\mathbf{x}}^{k-}$ can still be calculated using a linear matrix equation:

$$\mathbf{x}^k = \begin{bmatrix} \mathsf{A} & \mathbf{0} \\ \mathbf{0}^{\mathrm{T}} & 1 \end{bmatrix} \hat{\mathbf{x}}^{k-1} \tag{22}$$

The submatrix A is the same as that appearing in Eq. 10. Note that the process model has no means of adjusting η, only the filtering will modify this quantity.

Using the extended Kalman filtering (EKF) discussed previously, the filtering is based on the Jacobian matrix $\mathbb{F}$, which is a composite matrix:

$$\mathbb{F} = \frac{\partial \mathbf{f}}{\partial \mathbf{x}} = \begin{bmatrix} \mathsf{A} & \mathbf{a}_\eta \\ \mathbf{0}^{\mathrm{T}} & 1 \end{bmatrix} \qquad (\mathbf{a}_\eta)_i = \frac{\partial f_i}{\partial \eta} \tag{23}$$

Here, the elements of $\mathbf{a}_\eta$ are estimated by re-calculating $\mathbf{f}$ using $(\eta + \Delta\eta)$.

The results of the parameter estimation calculation are shown in Fig. 2(b). The same initial conditions were used as for the linear filter results in Fig. 2(a). The filtered values approach the true values (dotted lines) considerably sooner for the case of parameter estimation.

It is important to note that parameter estimation does not necessarily reduce uncertainty. The error bars in Figs. 2(a) and 2(b) are approximately the same size. (It is, however, interesting to note how small the error bars are, compared to the apparent variability in the measurements.)

The other important point is the significance of inherent model error. No amount of filtering can overcome a poor model. In the absence of parameter uncertainty, the filtering was working against a systemic bias. Parameter estimation removed this bias, and the filtered response approached the true value sooner.

6 - ELECTRO-DIFFUSION

The previous Fickian diffusion examples lay the basic foundation for service life calculations that are based on diffusion being the primary transport mode. The more sophisticated concrete service life models, however, incorporate the additional properties of electrolyte solutions. Although transport is primarily diffusion, the driving force is a gradient in the chemical potential μ. The flux $\mathbf{j}_i$ of the i-th species depends upon gradients in the species concentration c_i and the electrical potential ψ [11]:

$$\mathbf{j}_i^e = -D_i\left(1+\frac{\partial \ln y_i}{\partial \ln c_i}\right)\nabla c_i - z_i\,c_i\,u_i\,\nabla\psi \tag{24}$$

The coefficients are as follows: D_i is the self-diffusion coefficient; y_i is the molar activity coefficient; z_i is the valence; u_i is the electrochemical mobility; ψ is the electrical potential. The electrical field ψ can be determined from imposing a zero current constraint:

$$F\sum_i z_i\,\mathbf{j}_i = 0 \qquad F: \text{Faraday constant} \tag{25}$$

Given the initial and boundary conditions for the field variable $c(\mathbf{x},t)$, Eqs. 24 and 25 completely describe diffusive flux in bulk electrolyte. That is to say, Eq. 24 completely captures the electrochemical behavior of the solution.

Transport through a porous material having porosity θ and formation factor Υ can be expressed as a function of transport through the bulk electrolyte [12]:

$$\frac{\partial \theta c_i}{\partial t} = -\nabla \cdot \left(\frac{\mathbf{j}_i^e}{\Upsilon} \right) \tag{26}$$

This approach separates chemical effects from physical effects. As a result, the state vector is composed of the individual ionic species concentrations at computational elements and two additional numbers: the formation factor Υ and porosity θ.

7 - LABORATORY EXAMPLE

As an example of real porous materials filled with electrolyte, the data from a previous laboratory experiment [13] are analyzed using nonlinear Kalman filtering. The laboratory experiment is a divided cell diffusion test using a 6 mm thick porous alumina frit. The chamber on one side of the frit contains potassium iodide (KI), and the chamber on the other side of the frit contains a test solution. The frit is initially saturated with the KI, and the iodide concentration in each chamber is measured periodically. The two test solutions presented here are potassium chloride (KCl) and potassium hydroxide (KOH).

The initial value for the two transport coefficients, porosity and formation factor, were each determined using independent laboratory measurements, and are further refined using Kalman filtering. In theory, these values could have been roughly approximated and then refined using the Kalman filter. Because of the relatively small number of measurements in these examples, however, an accurate initial guess for the transport coefficients ensures convergence in a short time span. Because these were nonreactive frits, the transport coefficients should have remained constant in time. Here, the Kalman filter is used to predict the iodide concentration on each side of the frit and to refine the value for the formation factor.

As these are laboratory experiments, the complete inventory of ionic species present is known. Therefore, electroneutrality constrains the concentration of the ionic species; for M different ionic species present, only $M-1$ are independent. Therefore, a state vector that includes the concentrations of all the species is not practical because a numerical solution to the Jacobian $\mathbb{F}$ requires changing one value while holding all other values constant.

For this example, the state vector included the concentrations for only $M-1$ of the species present. That way, each of the $M-1$ species in the state vector could be varied, while keeping all the remaining concentrations constant. The nonlinear process function $\mathbf{f}(\mathbf{x})$ added a quantity of the remaining ionic species that ensured electroneutrality.

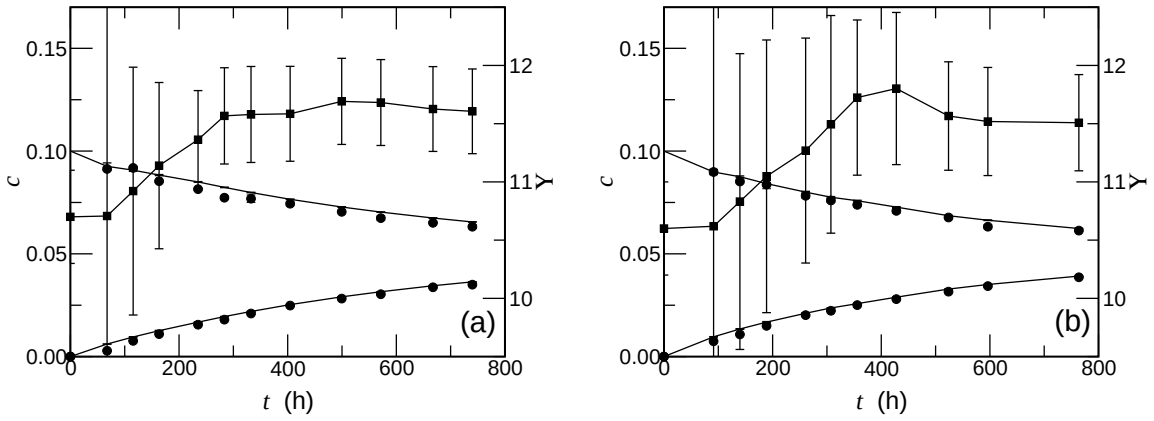

Figure 3: Concentration (c) data (filled circles) and formation factor (Υ) data (filled squares) for divided diffusion experiment using nonreactive ceramic frit. (a) KI/KCl system. (b) KI/KOH system.

The experimental measurements and filtered response for the KI/KCl and the KI/KOH systems are shown in Figs. 3(a) and 3(b), respectively. The measured concentrations on each side of the frit are denoted by filled circles, which often occlude the measurement error bars. The filtered concentrations are the lines following the measured

values. These filtered values have error bars denoting one standard deviation, but they are very small and difficult to see.

Also shown in the figures are the refined formation factor Υ values. These are shown as filled squares and error bars denote one standard deviation. In both systems, approximately 10 measurements were needed before the filtered formation factor converged to a steady value.

8 - MONITORING SCENARIO

The data presented in Fig. 3 help to illuminate the utility of Kalman filtering in a monitoring scenario. Not only can Kalman filtering be used to improve the predicted change in a system, but it can also be used to improve estimates of important parameters such as transport coefficients. These improved estimates are essential to ensuring accurate predictions of future performance.

As a schematic example to demonstrate the utility of Kalman filtering, consider the following fictitious scenario: A concrete structure is to go into service. One possible degradation mechanism depends upon the concentration of a particular mobile species. The monitoring strategy is to periodically test for the species and refine future predictions.

In practice, the performance of the structure will be estimated initially using the best available technology, often in the form of a computer model. Using parameter uncertainty, the model can be used to obtain an ensemble of performance predictions. Using any sensible means of quantifying the ensemble, one could make a statistical statement as to when the predicted performance of some fraction of the ensemble cross a critical threshold. The threshold could be any quantitative measure of performance. For example, threshold could be the concentration of a mobile species of interest.

For this monitoring scenario, a number of progressively increasing concentration thresholds are chosen at the outset, and monitoring is performed when the predicted concentration threshold crosses each successive critical value.

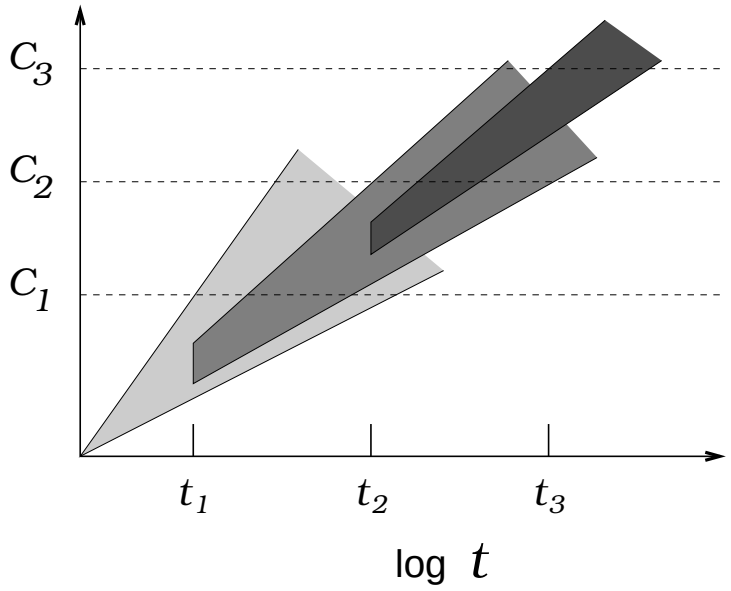

Figure 4: Fictitious monitoring scenario where monitoring is required as predetermined probabilities reach threshold limits.

This monitoring scenario is shown schematically in Fig. 4, with observation critical thresholds denoted C_1, C_2, etc. The initial ensemble of predicted responses is denoted by the lightest grey "fan" that originates at the origin. The region denotes the collection of ensemble calculations using parameter uncertainty. The upper limit of the region crosses the first threshold C_1 at time t_1. This is when the first monitoring occurs.

The result of the first measurement is to refine the model, from which a new ensemble of responses are calculated using the performance prediction model. This new ensemble is denoted by the medium grey region, which doesn't cross the next critical threshold C_2 until time t_2. At this time a second measurement is taken, and the model refined

again. The result of refinement leads to a new ensemble denoted by the darkest region, which first crosses the third threshold C_3 at time t_3. The process is then repeated as indicated.

9 - CONCLUSION

Based on these preliminary results, Kalman filtering appears to be a potentially useful tool for developing a rational monitoring strategy for concrete structures. One can effectively combine future model predictions and measurements in an unambiguous manner and achieve a smaller uncertainty than that for either model or observation individually.

Generally, filtering is most useful when the observable quantities have the greatest effect on the internal state variables. The best approach is to measure the internal variable of interest. Therefore, direct measurements of transport coefficients have a greater effect than concentration measurements. Also, the filtering requires a number of iterations before the filtered quantities begin to stabilize. Therefore, it may be prudent to perform a number of measurements early on in the process. Alternatively, these early measurements could be made on surrogate specimens with identical exposure as the service structure.

REFERENCES

[1] R. E. KALMAN, "A new approach to linear filtering and prediction problems," Journal of Basic Engineering - Trans. ASME, 82, 35–45 (1960).

[2] J.-P. DRÉCOURT, "Kalman filtering in hydrological modelling," Technical report, DHI Water & Environment, Hørsholm, Denmark (2003).

[3] D. MCLAUGHLIN, "An integrated approach to hydrologic data assimilation: Interpolation, smoothing, and filtering," Advances in Water Resources, 25, 1275–1286 (2002).

[4] P. VADDADI, T. NAKAMURA, and R. P. SINGH, "Inverse analysis for transient moisture diffusion through fiber-reinforced composites," Acta Materialia, 51, 177–193 (2003).

[5] L. A. AGUIRRE, B. O. S. TEIXEIRA, and L. A. B. TÔRRES, "Using data-driven discrete-time models and the unscented kalman filter to estimate unobserved variables of nonlinear systems," Physical Review E, 72 (2005).

[6] W. H. PRESS, B. P. FLANNERY, S. A. TEUKOLSKY, and W. T. VETTERLING, Numerical Recipes, Cambridge University Press, New York (1988).

[7] J. CRANK, The Mathematics of Diffusion, Oxford University Press, second edition (1975).

[8] H. W. SORENSON (Editor), Kalman Filtering: Theory and Application, IEEE Press (1985).

[9] S. J. JULIER and J. K. UHLMANN, "Unscented filtering and nonlinear estimation," Proc. IEEE, 92, 401–422 (2004).

[10] G. EVENSEN, "Sampling strategies and square root analysis schemes for the EnKF," Ocean Dynamics, 54, 539–560 (2004).

[11] I. RUBINSTEIN, Electro-Diffusion of Ions, Society for Industrial and Applied Mathematics, Philadelphia (1990).

[12] K. A. SNYDER, "The relationship between the formation factor and the diffusion coefficient of porous materials saturated with concentrated electrolytes: theoretical and experimental considerations," Concrete Science and Engineering, 3, 216–224 (2001).

[13] K. A. SNYDER and J. MARCHAND, "Effect of speciation on the apparent diffusion coefficient in nonreactive porous systems," Cement and Concrete Research, 31, 1837–1845 (2001).